SUPPLEMENTAL MATERIALS

Microrheology of highly crosslinked microtubule networks is dominated by force-induced crosslinker unbinding

By Yali Yang, Mo Bai, William S. Klug, Alex J. Levine, Megan T. Valentine

---

Appendix A: The relationship between crosslinker density and *R*

In principle the relationship between crosslinker density and the fraction of biotinylated tubulin *R* can be complex. For instance, when the concentration of biotinylated tubulin is sufficiently high, all filament-crossing points are saturated with binding sites so that changing *R* has no effect on the density of crosslinks. For this reason alone it is useful to estimate more carefully the relationship between *R* and the probability that the crossing of two microtubules provides at least one biotinylated tubulin on each filament in sufficient proximity to form a biotin-avidin crosslink. For the purposes of this analysis, we assume that there is sufficient streptavidin in solution so that this molecule is not the limiting reagent. We also assume that the biotinylated tubulin is incorporated randomly into the growing microtubules with no spatial correlations along the microtubule length.

We treat the two microtubules at a crossing point as two infinitely long cylinders of radius $\rho = 12.5$ nm arranged so as to touch at the origin of the coordinate system. We define the coordinate system so that the centre lines of the cylinders are both orthogonal to the *z*-axis. The first cylinder is parallel to the *x*-axis while the second is makes an angle of θ relative to the first one. The surfaces of these cylinders are then defined by the set of points

$$\vec{\ }_1 = x\hat{x} + \rho\sin\varphi_1\hat{y} + \rho(\cos\varphi_1 - 1)\hat{z} \tag{S.1}$$

$$\vec{\ }_2 = (st_x - \rho t_y \sin\varphi_2)\hat{x} + (st_y - \rho t_x \sin\varphi_2)\hat{y} + \rho(1+\cos\varphi_2)\hat{z}, \tag{S.2}$$

where $-\infty < x, s < \infty$, $(t_x, t_y) = (\cos\theta, \sin\theta)$ defines direction of the second cylinder with respect to the first, lying along the *x*-axis, and $\varphi_{1,2}$ are the azimuthal coordinates of cylinders one and two respectively. In terms of these variables, it is now a simple matter to compute the Cartesian distance between points on the two cylinders

$$L(x, s, \varphi_1, \varphi_2) = \left\| \vec{v}_1(x, \varphi_1) - \vec{v}_2(s, \varphi_1) \right\|. \tag{S.3}$$

We now determine the area on one cylinder where a biotinylated tubulin could be placed so that it could be crosslinked to some biotinylated tubulin on the other cylinder. To do this, we move out from the crossing point on cylinder one a distance *x* along a fixed azimuth φ_1, and

choose a distance s and azimuthal coordinate φ_2 on cylinder two to minimize the distance between that point on cylinder one and some point on cylinder two using Eq. (S.3). By determining the locus of points where that minimum distance is equal to or less than the maximum allowable distance for streptavidin binding (which we take to be 5 nm), we determine the area on a cylinder over which a biotinylated tubulin may form a crosslink. We refer to this as the potential crosslinking area on a cylinder.

Taking the area of a tubulin dimer to be 4 nm×8 nm, we may simply compute the number N of such dimers within the potential crosslinking area. Now, a crosslink can form if a tubulin dimer within the potential crosslinking area and its corresponding dimer on the other microtubule are both biotinylated. The probability of this is R^2. Given the relative size of a tubulin dimer and the streptavidin linker, we may assume that each biotinylated tubulin dimer can form a crosslink only with one corresponding dimer on the other microtubule. The probability of there being at least one such crosslink is then given by

$$\text{Prob} = \sum_{m=1}^{N} \frac{N!}{(N-m)!\,m!} R^{2m}(1-R^2)^{N-m}. \qquad \text{(S.4)}$$

Of course, the size of the potential crosslinking area depends on the crossing angle of the two microtubules in question. As that angle approaches zero (the case of bundled filaments) the area diverges. But, since we are interested in crosslinks that form a space-filling and stress-bearing network, bundling is not relevant to this calculation. Performing this computation of the size of the potential crosslinking areas for two different microtubule-crossing angles: $\theta = \pi/2, \pi/12$, we find them to be $2.9\,\rho^2$ and $10.2\,\rho^2$ respectively. We expect that these crossing angles are in the range relevant for forming the network. Converting these areas to N, the number of tubulin dimers involved, and using Eq.(S4) we find that the probability of a crosslink occurring at $R = 0.06$ is 5% for $\theta = \pi/2$, increasing to 16.5% for more nearly aligned filaments crossing at an angle of $\theta = \pi/12$. At a concentration of $R = 0.125$ we find the crosslinking probability at a crossing point is now 50% for the $\theta = \pi/2$ crossing points, and about 90% for the lower angle crossings – $\theta = \pi/12$. Increasing the concentration of biotinylated tubulin to R=0.5, these probabilities approach unity, suggesting that the R=0.5 is near the saturation concentration.

It should be pointed out that these calculations produce overestimates of the crosslinker concentration for at least two reasons. First, if the two microtubules do not exactly touch at their point of nearest approach, as assumed here, the potential crosslinking area decreases further for all crossing angles. Second, it is likely that, due to steric constraints, not all biotin molecules are available for crosslinking. For example, assuming that only half of the biotin is available converts an $R = 0.125$ sample to a $R = 0.06$ one; now, instead of half of the crossing points having crosslinks, only one in twenty is expect to have one. Given these uncertainties, the conclude by making the following observations: (1) The range of R used in the experiments is

reasonably expected to be in below the saturation regime so that changes in R should result in changes in the number of crosslinks in the network. (2) Assuming that only about half of biotin is chemically available, it is reasonable to conclude that the experimental range of R encompasses networks from fairly sparse crosslinking (one in ~20 crossing points have crosslinkers) all the way up to high crosslinking concentrations. (3) In fact, the crosslinker saturation regime occurs at values of R not significantly larger than the maximum used, $R = 0.5$, suggesting that the most densely crosslinked networks tested represent ones at nearly maximum crosslink density.

Supplementary Figures.

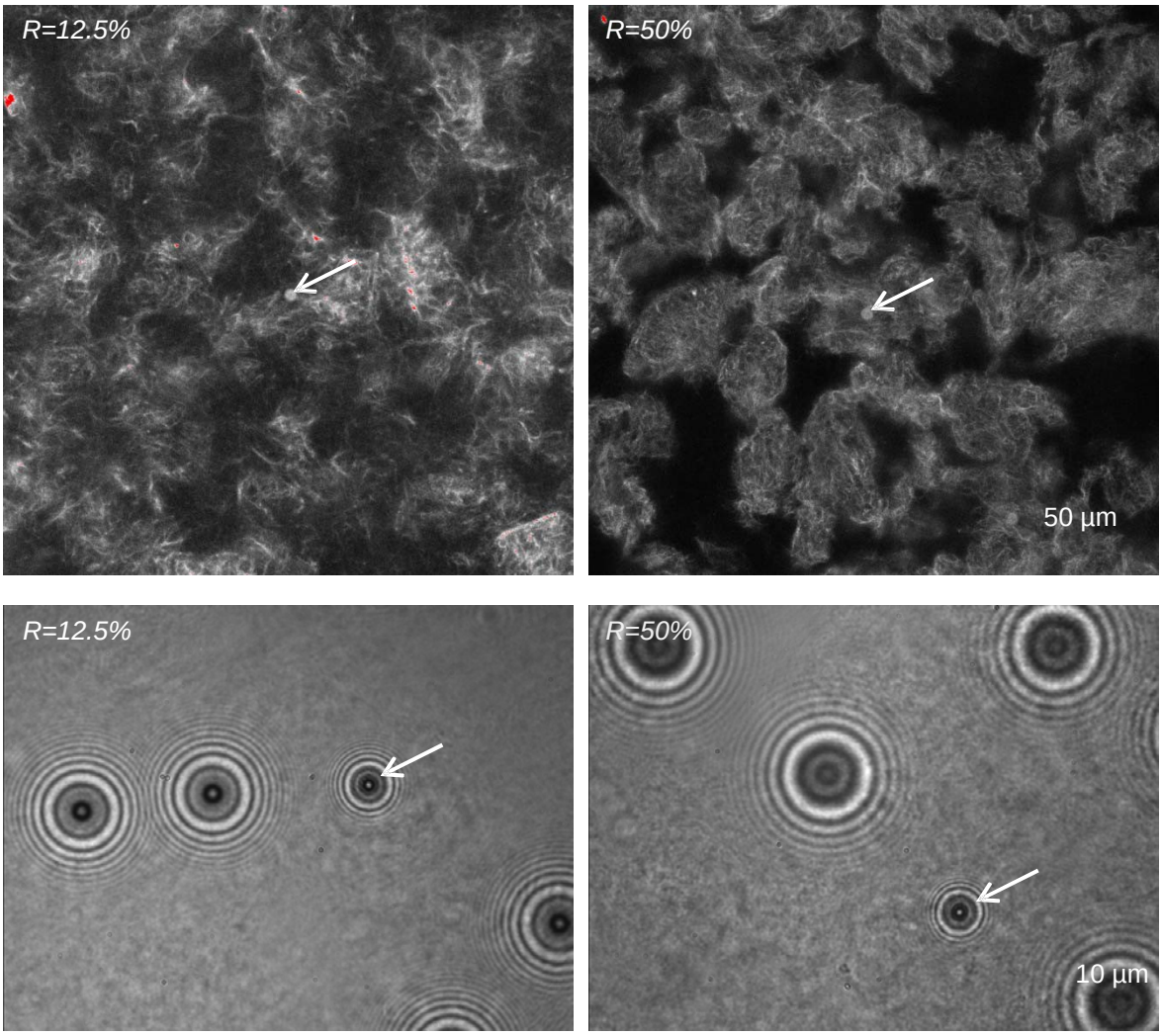

Figure S1: Representative images of crosslinked MT networks embedded with magnetic beads obtained using confocal fluorescence microscopy (upper) and magnetic tweezers (lower). Total tubulin concentration is 25 µM. Networks are crosslinked through streptavidin biotin bonds, and the degree of crosslinking, *R*, is controlled by varying the ratio of biotin-labelled tubulins to total tubulin. The structures of crosslinked MT networks are highly heterogeneous. Magnetic beads (white arrows) are mostly found in areas with dense structures or in the border regions between areas with sparse and dense structures.Note that the upper and lower images are collected independently on two different instruments, and do not show the same field of view.Red pixels indicate that the pixel intensity exceeds the maximum value.

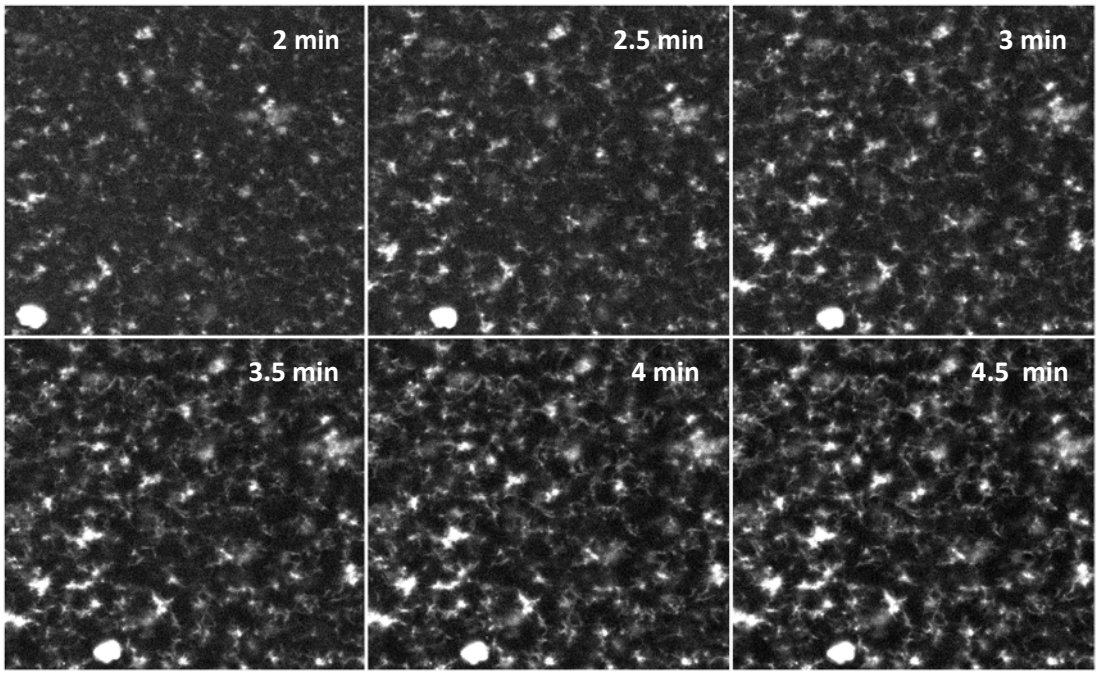

Figure S2: Time-lapsedfluorescence confocal images of crosslinked MT network, with R = 25%, formed at 30˚C, taken every 30 seconds after the sample is loaded into the temperature controlled chamber. To allow the MT growth stage to be observed, the 3-minute preincubation step is omitted and streptavidin is present in solution at the start of MT assembly. Time stamps are shown in the upper right of each frame. At 2 min (when the recording starts),nucleation centres and thin and short MT filaments have already formed. Flow of the networks is almost stopped at 3.5 min. At longer times, free tubulin proteins and tubulin aggregates (seen as bright pixels in the background) are added to existing nucleation centres to make thicker and longer MT filaments that are connected throughout the sample. Movie of network formation is included as **Supplementary Movie 1**.

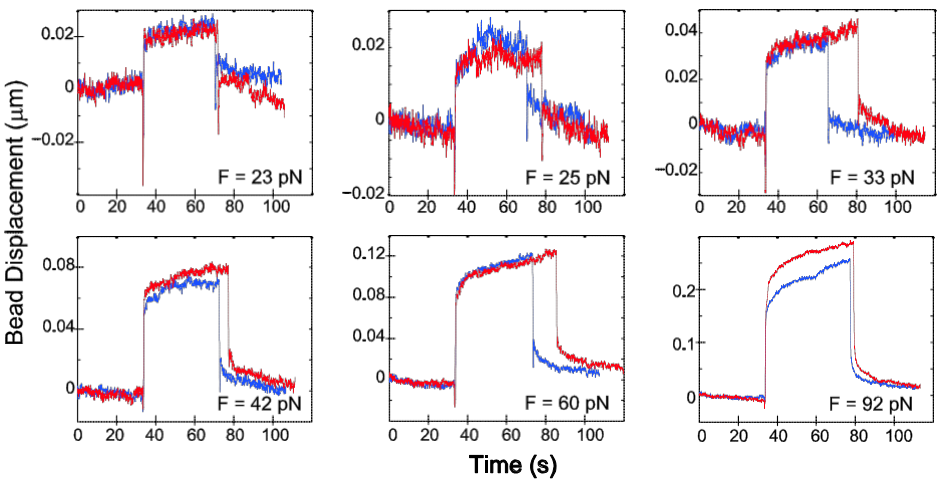

Figure S3: Individual traces of bead displacement versus time as forces are ramped up (blue) or ramped down (red) from the maximum value of 151 pN, for a network formed from 25 μM total tubulin and with R = 50%. The general features for the traces are similar for the ramp up and ramp down cases, indicating little (if any) hysteresis. Only at the highest forces >90 pN do we consistently observe a softer network for the ramp down (i.e. the red curve is consistently higher than the blue curve because the bead moves further under the same force condition.) In some cases, a small "drift" can be observed prior to application of force. This is not due to artefactual motion of the system, as all traces have already been corrected for mechanical/thermal drift through subtraction of the motion of the reference bead. Rather, this bead motion arises from actual network dynamics under repeated loading. In order to optimize data throughput for these fragile and time-sensitive samples, we choose a waiting time between loading cycles of ~50-100 seconds. Because network dynamics occur on all timescales, including very long ones, it is not possible for the network to completely relax during the finite timescale of our measurement. However, the observed particle motion is a very minor contribution to the force-induced motions we observe, and does not affect any of our conclusions.

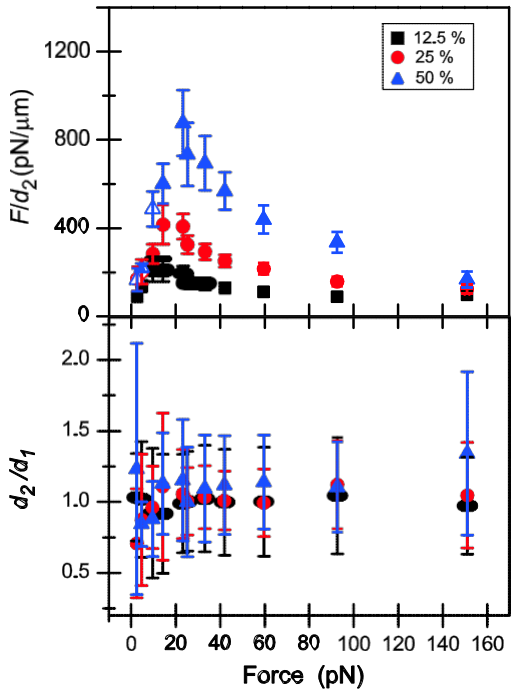

Figure S4: (a) Stiffness of crosslinked MT networks, given by F/d_2 as a function of force. The force-off stiffness F/d_2 shows stiffening at low forces and softening at high forces consistent with force-on stiffness F/d_1. (b) The value of F/d_2 and F/d_1 are roughly the same within errors for the force range studied.

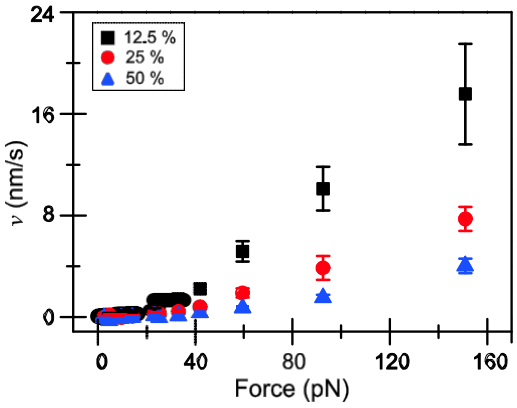

Figure S5: The velocity is plotted as a function of force. Using a lin-lin plot, we demonstrate that the creep velocity v becomes significant only for forces above F_c.

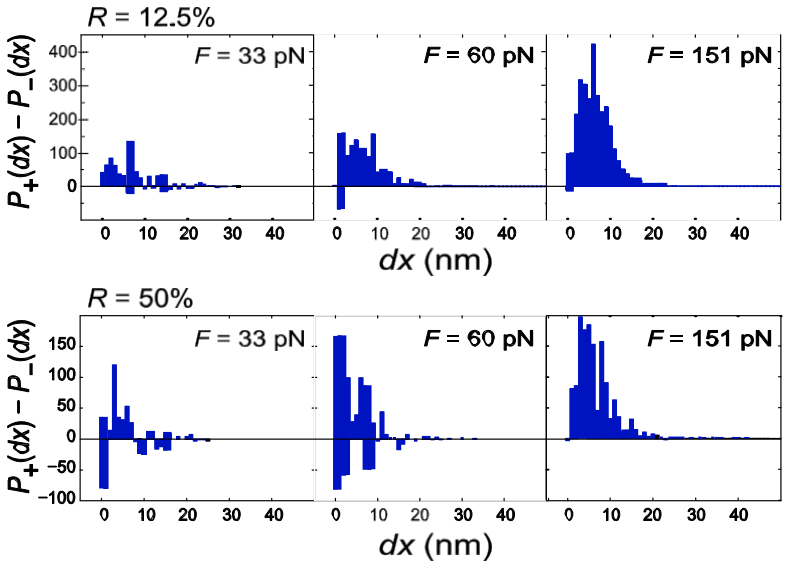

Figure S6: The difference $P_{+}(dx) - P_{-}(dx)$ gives the distribution of 'excess' fluctuations in the direction of applied force, which we attribute to bond breakage events. Here, $P_{+}(dx) - P_{-}(dx)$ is plotted for R = 12.5% (upper) and R = 50% (lower) and F = 33 pN, 60 pN, and 151 pN. Distributions for R = 25% are shown in Figure 5.